$\bar{D}^0D^{0*}$ ($D^0\bar{D}^{0*}$) system in QCD-improved many body potential *

M. Imran Jamil[1] Bilal Masud[2] Faisal Akram[2] S. M. Sohail Gilani[2;1)]

[1] University of Management and Technology, Lahore, Pakistan

[2] Centre For High Energy Physics, Punjab University, Lahore(54590), Pakistan

Abstract: For a system of current interest (composed of charm, anticharm and a pair of light quarks), we show trends in phenomenological implications of QCD-based improvements to a simple quark model treatment. We employ a resonating group method to render this difficult four-body problem manageable. We use a quadratic confinement so as to be able to improve beyond the Born approximation. We report the position of the pole corresponding to the $\bar{D}^0D^{0*}$ molecule for the best fit of a model parameter to the relevant QCD simulations. We point out the interesting possibility that the pole can be shifted to 3872 MeV by introducing another parameter I_0 that changes the strength of the interaction in this one component of $X(3872)$. The revised value of this second parameter can guide future trends in modeling of the full exotic meson $X(3872)$. We also report the changes with I_0 in the S-wave spin averaged cross sections for $\bar{D}^0D^{0*} \longrightarrow \omega J/\psi$ and $\bar{D}^0D^{0*} \longrightarrow \rho J/\psi$. These cross sections are important regarding the study of QGP (quark gluon plasma).

Keywords: meson-meson interaction, resonating group method, quark potential model, X(3872)

PACS: 13.75.Lb, 14.40.Lb, 12.39.Jh **DOI:** 10.1088/1674-1137/41/1/013103

1 Introduction

Considering the difficulties in solving quantum chromodynamcis (QCD) for the relevant energies, hadron phenomenology and hadron-hadron scattering is studied mostly through models or effective Lagrangian densities. But as far as possible, continuum hadronic models should agree with lattice simulations of QCD and give phenomenological implications which have a good comparison with the corresponding hard experimental results. For multiquark systems, a common approach, which has a fairly good phenomenological record, is the sum of pair-wise interaction model [1–13]. The need for improvement in it is indicated even phenomenologically by noting that this model predicts color van der Waals interaction of the inverse-power type between separated hadrons, for which there is no experimental evidence. At the quark level, good lattice-based improvements [14–17] to this sum of two-body potential model are available which modify it at large distances. These improvements introduced a space dependent form factor f (appearing in Eqs. (9), (10) and (11) below) in off-diagonal elements in the overlap, potential and kinetic energy matrices of the model. The additional parameter in f minimizes the difference between the two quark two antiquark binding in the improved model to the binding resulting from relevant lattice-generated QCD simulations by UKQCD [18–21]. The exponential form of f keeps the model in agreement with the pair-wise interaction model in the small distance limit while getting a fairly good agreement to the QCD simulations and solving the van der Waals problem.

It is necessary to find testable implications of these improvements at the meson level in form of multiquark energies (binding) and meson-meson cross-sections. Without these improvements, the $\bar{D}^0D^{0*}$ and its coupling to $\omega J/\psi$ or $\rho J/\psi$ has been studied [7, 8, 22]. Refs. [7, 8] report the resulting $\rho J/\psi$ to $\bar{D}^0D^{0*}$ cross sections, along with many others. Ref. [22] reports meson-meson potential and eigenvalues for $D\bar{D}^*$ and $B\bar{B}^*$ four-quark states and find molecular states in the resulting combinations. We are now calculating revised implications for the $\bar{D}^0D^{0*}$ system. These implications address some experimental issues of wide interest, for example understanding exotic mesons [23–25]. An important such state is the meson X(3872) which is now generally considered [26–32] as a mixture of $\bar{D}^0D^{0*}$, D^+D^{-*} and $c\bar{c}$. Any

Received 27 June 2016, Revised 22 September 2016

∗ BM and FA acknowledge the support of PU research (D/605/Est.I Sr. 20 Project 2014-15, D/34/Est.1 Sr. 109 Project 2013-14), SG is thankful to the Higher Education Commission (HEC) of Pakistan for its financial support through (17-5-4(Ps3-128) HEC/Sch/2006)

1) E-mail: msgilani2005@gmail.com

Content from this work may be used under the terms of the Creative Commons Attribution 3.0 licence. Any further distribution of this work must maintain attribution to the author(s) and the title of the work, journal citation and DOI. Article funded by SCOAP[3] and published under licence by Chinese Physical Society and the Institute of High Energy Physics of the Chinese Academy of Sciences and the Institute of Modern Physics of the Chinese Academy of Sciences and IOP Publishing Ltd

effort to understand it, thus, should understand quantities depending upon its components. A direct lattice QCD study of it would have to calculate many Wilson loops before arriving at any conclusion. A more manageable route could be to make separate models of its components, find out their consequences and then combine the models to understand X(3872). Our work is the first step in this scheme; we take up the $\bar{D}^0D^{0*}$ system whose flavor content has an overlap with both isovector $\rho J/\psi$ and isoscalar $\omega J/\psi$ and we study its coupling to both channels.

Ref. [33] addresses the possibility that X(3872) is a molecular bound state of neutral charm mesons and Refs. [34–38] assume so. Ref. [4] says that $\bar{D}^0D^{0*}$ to $\omega J/\psi$ (and $\rho J/\psi$) interaction is needed to understand models of X(3872). $\bar{D}^0D^{0*} \longrightarrow \omega(\rho)J/\psi$ scattering is needed to understand the final state interaction in the X(3872) decaying to $J/\psi\rho$ or $J/\psi\omega$ through the intermediate $\bar{D}^0D^{0*}$. Refs. [39, 40] describe the role of this final state interaction through the effective Lagrangian approach. We present results that may have implications for these final state interactions while being closer to QCD in giving a quark level description. Refs. [41, 42] use the sub-process $\bar{D}^0D^{0*} \longrightarrow \bar{D}^0D^{0*}$ for the final state interaction in the net $B \longrightarrow \bar{D}^0D^{0*}K$ process. Our comments also apply to this channel and we show below our results for $\bar{D}^0D^{0*} \longrightarrow \bar{D}^0D^{0*}$ scattering as well. In a recent paper, Braaten and Kang [43] say that "in case of 1^{++} quantum numbers of X(3872), effects of scattering between $\omega J/\psi$ and charm meson pairs could be significant." Moreover, $\bar{D}^0D^{0*} \longrightarrow \omega(\rho)J/\psi$ scattering is needed for studying the effect of final state interactions between the comovers in relativistic heavy ion collision experiments [44].

For the $\bar{D}^0D^{0*}$ system, another improvement beyond the quark-antiquark pair-wise interaction implemented is Ref. [4]. This adds a point-wise meson interaction to the coupling resulting from one gluon exchange and calculates the resulting $\bar{D}^0D^{0*}$ to $\omega J/\psi$ scattering amplitudes. We, in this paper, present $\bar{D}^0D^{0*}$ to $\omega J/\psi$ and $\rho J/\psi$ cross-sections along with an analysis of $\bar{D}^0D^{0*}$ binding resulting from the f model [14, 15, 17] that better fits the available QCD simulations than the one gluon exchange model. In a previous work [45], we used the Born approximation to calculate the meson-level consequences of the most developed geometrical form of the f factor. In the present paper, we use a resonating group formalism to avoid the Born approximation used in Refs. [45–48] for meson-meson scattering and thus the reported results can be compared with the Born approximation [49]. This is essential to be able judge how good the approximation is. To get analytic expressions for the resulting scattering amplitudes, now we use a quadratic confinement and a simpler form of the f factor. We incorporate the spin and flavour dependence. A similar realistic meson-meson treatment for lighter quarks was published earlier [50]. We now address a system ($\bar{D}^0D^{0*}$) of current interest and give a much more thorough analysis of the meson-meson binding. Moreover, we include the meson-meson cross-sections that are not in Ref. [50] at all.

These cross sections can be useful in experimental studies of quark-gluon plasma (QGP) in relativistic heavy ion collisions. One of the promising signatures of QGP in heavy ion collision experiments is the suppression of J/Ψ caused by color Debye screening. However, the observed suppression may be affected by the interaction of J/Ψ with the comoving hadrons, mainly π and ρ mesons, after the hadronization of QGP. The effect of the interactions with the comovers can be significant as the density of these mesons is very high. Thus an estimate of these cross sections can help in identifying any contribution of QGP in the observed production rate of J/Ψ in heavy ion collision experiments.

This paper is organized as follows. In Section 2 we have specified our $q^2\bar{q}^2$ Hamiltonian and written the spin and flavor wave functions and the form of the position wave function of our system. The section ends with the integral equations for the unknown position factors of our total wave function, as in a resonating group formalism. In Section 3, we solve our integral equations for the amplitudes of transition between two channels of our multiquark system. In Section 4 we report the best fit values of the parameters used in our formalism along with describing how they are fixed. In Section 5, we present our results for the scattering cross-sections and bindings and give our conclusions.

2 The Hamiltonian matrix and the wave functions

We use the adiabatic approximation to first define the potential for fixed positions of two quarks and two antiquarks. The model we use (that of Ref. [15], with position dependence as that of the model I_a in Ref. [14]) improves the kinetic, potential and overlap matrices in the color basis

$$|1\rangle_c = |1_{1\bar{3}}1_{2\bar{4}}\rangle_c, \qquad |2\rangle_c = |1_{1\bar{4}}1_{2\bar{3}}\rangle_c. \tag{1}$$

They fit to the lattice simulations a parameter k_f introduced in the off-diagonal position dependent elements of these matrices, while keeping the small distance limit of the model agreeing to the pair-wise model. To avoid the Born approximation, we had to use the simplest form

$$f = \exp\left(-b_s k_f \sum_{i<j} r_{ij}^2\right). \tag{2}$$

in the off-diagonal elements that is used in the otherwise more developed model version in Ref. [15].

In the next step of the adiabatic approximation, we calculate the quark position wave functions. For this, we start by writing our total state vector as a sum over k of the product of the gluonic states $|k\rangle_g$, known spin and flavor states and the corresponding quark position wave function $\boldsymbol{\Psi}^k(\boldsymbol{r}_1,\boldsymbol{r}_2,\boldsymbol{r}_{\bar{3}},\boldsymbol{r}_{\bar{4}})$. $|k\rangle_g$ is defined as the QCD eigenstate that approaches the corresponding colour state $|k\rangle_c$ in the small distance limit. The position dependence of the overlaps and potential energy matrices in the $\{|k\rangle_g\}$ basis are taken from the abovementioned Refs. [14, 15]. For the kinetic energy matrices we use the non-relativistic prescriptions used in Ref. [16]; there it is justified through the effective hadron Hamiltonian [51] in (space-)lattice QCD. To these we add (after multiplying the appropriate identity matrices) the sum of the corresponding constituent quark masses m_i $(i=1,2,\bar{3},\bar{4})$, fixed [52] to meson spectroscopy, to get the total meson-meson Hamiltonian matrix; this semi-relativistic prescription is already used in Refs. [1, 2, 16, 50]. The resulting matrices are improvements to the matrices in the basis of Eq. (1) of the Hamiltonian appearing in Ref. [1], i.e.

$$\hat{H}=\sum_{i=1}^{\bar{4}}\left[m_i+\frac{\hat{P}_i^2}{2m_i}\right]+\sum_{i<j}v(\boldsymbol{r}_{ij})\boldsymbol{F}_i.\boldsymbol{F}_j. \tag{3}$$

$\boldsymbol{F}_i$ is the set of color matrices (of $SU(3)_c$) for the ith particle. $\boldsymbol{F}$ has 8 components $F_a=\dfrac{\lambda_a}{2}$ for a quark and for an anti quark $F_a=-\dfrac{\lambda_a^*}{2}$, $a=1,2,3,\cdots,8$. For using our analytic formalism beyond the Born approximation we employed a simple harmonic potential already used in Refs. [1, 16, 50]

$$v(\boldsymbol{r}_{ij})=v_{ij}=Cr_{ij}^2+\bar{C}\ \text{with}\ i,j=1,2,\bar{3},\bar{4}, \tag{4}$$

rather than more sophisticated forms of Refs. [22, 53, 54]. Our neglect of the hyperfine interaction is less serious in $\bar{\mathrm{D}}^0\mathrm{D}^{0*}\to\omega(\rho)\mathrm{J}/\psi$ processes; Ref. [4] shows that this amplitude is dominated by the confinement interaction.

This specifies our formula of color interactions between different quarks. The explicit color dependent factor in it is $\boldsymbol{F}_i.\boldsymbol{F}_j$ and that is flavor independent, consistent with the color charge on a quark on any flavor being same. Its quadratic confining coefficient $Cr_{ij}^2+\bar{C}$ is to replace the more sophisticated forms of Refs. [22, 53, 54], in which the coefficient of the confining term, the QCD string tension, is everywhere taken to be flavor independent; the string tension models the energy density of the gluonic field originating from color charges, and color charges are the same for each flavor. The confining term we use is Cr_{ij}^2 and its coefficient C is accordingly taken to be flavor independent. This gluonic field energy density is calculated in the lattice QCD simulations of Ref. [55] and this work advocates a flavor independent string tension. The constant term $\bar{C}$ is added to the flavor dependent sum of constituent quark masses in our actual formulas for meson masses, for example in Eq. (43) below.

As in the resonating group method, we factorize Ψ^k into known and unknown factors to utilize the well known SHO position wave functions $\xi_k(\boldsymbol{y}_k)$ and $\zeta_k(\boldsymbol{z}_k)$ within each quark antiquark subsystem

$$\begin{aligned}&|\Psi(\boldsymbol{r}_1,\boldsymbol{r}_2,\boldsymbol{r}_{\bar{3}},\boldsymbol{r}_{\bar{4}};g)\rangle\\&=\sum_{k=1}^{2}|k\rangle_g|k\rangle_f|k\rangle_s\Psi_c(\boldsymbol{R}_c)\chi_k(\boldsymbol{R}_k)\xi_k(\boldsymbol{y}_k)\zeta_k(\boldsymbol{z}_k).\end{aligned} \tag{5}$$

$|k\rangle_f$ are the flavor states and $|k\rangle_s$ are the spin states. Here $\boldsymbol{R}_c$ is the c.m. position vector. The inter-cluster vector $\boldsymbol{R}_k$ and in-cluster vectors $\boldsymbol{y}_k$ and $\boldsymbol{z}_k$ are shown in Figs. 1 and 2, which also define the topologies $k=1,2$. For example,

$$\boldsymbol{R}_1=\frac{(\boldsymbol{r}_1+r\boldsymbol{r}_{\bar{3}}-r\boldsymbol{r}_2-\boldsymbol{r}_{\bar{4}})}{(1+r)}. \tag{6}$$

Here $r=\dfrac{m_c}{m}$, with m,m_c being the constituent masses of the light (up or down) and charm quarks respectively.

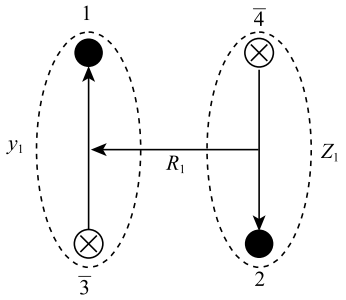

Fig. 1. Topology 1

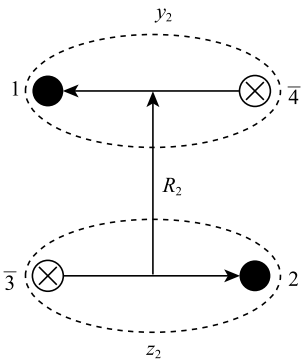

Fig. 2. Topology 2

The sizes d_{k1} and d_{k2} of the known quark antiquark clusters are also parameters of our model. d_{k1} is defined

by

$$\xi_k(\boldsymbol{y}_k)=\frac{1}{(2\pi d_{k1}^2)^{\frac{3}{4}}}\exp\Big(\frac{-\boldsymbol{y}_k^2}{4d_{k1}^2}\Big). \tag{7}$$

d_{k2} replaces d_{k1} in $\zeta_k(\boldsymbol{z}_k)$. The unknown inter-cluster factor $\chi_k(\boldsymbol{R}_k)$ is our variational function found by solving the integral Eq. (8) for it. To get this equation, we set the overlap of an arbitrary variation $|\delta\Psi\rangle$, in $|\Psi\rangle$ of Eq. (5), with $(\hat{H}-E_c)|\Psi\rangle$ as zero and reading off the coefficients of the arbitrary variations $\chi_k(\boldsymbol{R}_k)$ with $k=1,2$. This gives

$$\begin{aligned}&\sum_{l=1}^{2}\int \mathrm{d}^3\boldsymbol{y}_k\mathrm{d}^3\boldsymbol{z}_k\ {}_f\langle k|l\rangle_f\ {}_s\langle k|l\rangle_s\\&\xi_k(\boldsymbol{y}_k)\zeta_k(\boldsymbol{z}_k)_g\langle k|\hat{H}-E_c|l\rangle_g\chi_l(\boldsymbol{R}_l)\xi_l(\boldsymbol{y}_l)\zeta_l(\boldsymbol{z}_l)=0.\end{aligned} \tag{8}$$

The trivial integration over the c.m. position $\boldsymbol{R}_c$ could be performed to give a finite result (implied in the above equation) using, say, a box normalization. It is to be noted that our total meson-meson Hamiltonian is an identity operator in the flavor and spin basis because it differs from that in Eq. (3) only through the position dependent f and we are neglecting the spin-spin hyperfine interaction.

We use ${}_g\langle k|l\rangle_g$, ${}_g\langle k|\hat{V}|l\rangle_g$ and ${}_g\langle k|\hat{K}|l\rangle_g$ of Refs. [15, 16] to get the ${}_g\langle k|\hat{H}-E_c|l\rangle_g$ required in Eq. (8). These form the matrices:

$$N\equiv\{N_{kl}\}\equiv\{{}_g\langle k\,|\,l\rangle_g\}=\begin{pmatrix}1&\frac{1}{3}f\\\frac{1}{3}f&1\end{pmatrix}, \tag{9}$$

$$\begin{aligned}V&\equiv\{V_{kl}\}\equiv\{{}_g\langle k\,|\,\hat{V}\,|\,l\rangle_g\}\\&=\begin{pmatrix}-\frac{4}{3}(v_{1\bar{3}}+v_{2\bar{4}})&\frac{4}{9}f(v_{12}+v_{\bar{3}\bar{4}}-v_{1\bar{3}}-v_{2\bar{4}}-v_{1\bar{4}}-v_{2\bar{3}})\\\frac{4}{9}f(v_{12}+v_{\bar{3}\bar{4}}-v_{1\bar{3}}-v_{2\bar{4}}-v_{1\bar{4}}-v_{2\bar{3}})&-\frac{4}{3}(v_{1\bar{4}}+v_{2\bar{3}})\end{pmatrix}\end{aligned} \tag{10}$$

$$K\equiv\{K_{kl}\}\equiv{}_g\langle k|\hat{K}|\ l\rangle_g=N(f)^{\frac{1}{2}}_{k,l}\left(\sum_{i=1}^{\bar{4}}-\frac{\nabla_i^2}{2m}\right)N(f)^{\frac{1}{2}}_{k,l}. \tag{11}$$

For $\bar{\mathrm{D}}^0\mathrm{D}^{0*}$ (chosen as channel 1 with $k=1$), the total spin is 1. Angular momentum conservation tells that in the quark exchanged channels ($\omega\mathrm{J}/\psi$ and $\rho\mathrm{J}/\psi$ corresponding to $k=2$) the total spin should be 1. These spin states are denoted by

$$|1\rangle_s=|P_{1\bar{3}}V_{2\bar{4}}\rangle \tag{12}$$

$$|2\rangle_s=|V_{1\bar{4}}V_{2\bar{3}}\rangle, \tag{13}$$

where P represents a pseudo-scalar and V represents a vector meson. We utilize the rotational symmetry of our problem to write each of these S=1 states as $\frac{1}{\sqrt{3}}(|1,1\rangle+|1,0\rangle+|1,-1\rangle)$ with the second label as the S_z quantum number. We then use the completeness of the meson and then quark spins, along with the required Clebsch-Gordan coefficients, to arrive at the following for ${}_s\langle k|l\rangle_s$ in Eq.(8)

$${}_s\langle 1|2\rangle_s={}_s\langle 2|1\rangle_s=\frac{1}{\sqrt{2}}. \tag{14}$$

The flavor content of our channel-1 is unique

$$|1\rangle_f=|\bar{c}u\rangle|c\bar{u}\rangle. \tag{15}$$

For the second channel, it depends on our choice of mesons in it:

$$|2\rangle_f=\begin{pmatrix}\frac{1}{\sqrt{2}}|u\bar{u}+d\bar{d}\rangle|c\bar{c}\rangle&\text{for}&\omega\mathrm{J}/\psi&\text{mesons}\\\frac{1}{\sqrt{2}}|u\bar{u}-d\bar{d}\rangle|c\bar{c}\rangle&\text{for}&\rho\mathrm{J}/\psi&\text{mesons}\end{pmatrix}. \tag{16}$$

This gives in Eq. (8)

$${}_f\langle 1|2\rangle_f=\frac{1}{\sqrt{2}} \tag{17}$$

for both $\omega\mathrm{J}/\psi$ and $\rho\mathrm{J}/\psi$ in channel 2.

3 Solving the integral equations

When Eqs. (9)–(11) and Eqs. (14), (17) are substituted in Eq. (8), we get the following equation

$$\begin{aligned}&\int \mathrm{d}^3\boldsymbol{R}'_k\Big[\boldsymbol{K}_{kk}(\boldsymbol{R}_k,\boldsymbol{R}'_k)+\boldsymbol{V}_{kk}(\boldsymbol{R}_k,\boldsymbol{R}'_k)\\&+\left(\sum_{i=1}^{\bar{4}}m_i-E_c\right)\boldsymbol{N}_{kk}(\boldsymbol{R}_k,\boldsymbol{R}'_k)\Big]\chi_k(\boldsymbol{R}'_k)\\&+\int_{l\neq k}\mathrm{d}^3\boldsymbol{R}_l\Big[\boldsymbol{K}_{kl}(\boldsymbol{R}_k,\boldsymbol{R}_l)+\boldsymbol{V}_{kl}(\boldsymbol{R}_k,\boldsymbol{R}_l)\\&+\left(\sum_{i=1}^{\bar{4}}m_i-E_c\right)\boldsymbol{N}_{kl}(\boldsymbol{R}_k,\boldsymbol{R}_l)\Big]\chi_l(\boldsymbol{R}_l)=0,\end{aligned} \tag{18}$$

with the kernels $\boldsymbol{K}_{kl}(\boldsymbol{R}_k,\boldsymbol{R}'_l)$, $\boldsymbol{V}_{kl}(\boldsymbol{R}_k,\boldsymbol{R}'_l)$ and

$\boldsymbol{N}_{kl}(\boldsymbol{R}_k,\boldsymbol{R}'_l)$ defined, in the notation of Eq. (8), by

$$\int \mathrm{d}^3\boldsymbol{y}_k\mathrm{d}^3\boldsymbol{z}_k\xi_k(\boldsymbol{y}_k)\zeta_k(\boldsymbol{z}_k)K_{kl}\,\chi_l(\boldsymbol{R}_l)\xi_l(\boldsymbol{y}_l)\zeta_l(\boldsymbol{z}_l)$$
$$=\frac{2}{\delta_{kl}+1}\int \mathrm{d}^3\boldsymbol{R}'_l\boldsymbol{K}_{kl}(\boldsymbol{R}_k,\boldsymbol{R}'_l)\chi_l(\boldsymbol{R}'_l) \tag{19}$$

$$\int \mathrm{d}^3\boldsymbol{y}_k\mathrm{d}^3\boldsymbol{z}_k\xi_k(\boldsymbol{y}_k)\zeta_k(\boldsymbol{z}_k)V_{kl}\,\chi_l(\boldsymbol{R}_l)\xi_l(\boldsymbol{y}_l)\zeta_l(\boldsymbol{z}_l)$$
$$=\frac{2}{\delta_{kl}+1}\int \mathrm{d}^3\boldsymbol{R}'_l\boldsymbol{V}_{kl}(\boldsymbol{R}_k,\boldsymbol{R}'_l)\chi_l(\boldsymbol{R}'_l) \tag{20}$$

$$\int \mathrm{d}^3\boldsymbol{y}_k\mathrm{d}^3\boldsymbol{z}_k\xi_k(\boldsymbol{y}_k)\zeta_k(\boldsymbol{z}_k)N_{kl}\,\chi_l(\boldsymbol{R}_l)\xi_l(\boldsymbol{y}_l)\zeta_l(\boldsymbol{z}_l)$$
$$=\frac{2}{\delta_{kl}+1}\int \mathrm{d}^3\boldsymbol{R}'_l\boldsymbol{N}_{kl}(\boldsymbol{R}_k,\boldsymbol{R}'_l)\chi_l(\boldsymbol{R}'_l). \tag{21}$$

The factor $\dfrac{2}{\delta_{kl}+1}$ takes care of the off-diagonal spin and flavor overlap factors, both $=\dfrac{1}{\sqrt{2}}$. The spatial integrations on the left hand side of Eqs. (19–21) and resulting kinetic energy, interaction and normalization kernels are reported in Appendix A. A comparison of kernels themselves can have a dynamical result; Ref. [56] tells that if the interaction kernel is proportional to the normalization kernel, the interaction does not contribute to the interaction between mesons. Eqs. (A2) and (A8) in Appendix A show that such is the case in our calculations for a single channel completely described by the diagonal terms in kernels in these equations. For quadratic confinement in the one channel approximation Ref. [56] also gets the same result for the interaction between the mesons. But with an improved model for the two channel meson-meson interaction our full results are obtained by substituting diagonal as well as off-diagonal terms in Eq. (18) and in our case the interaction kernel is not proportional to the normal kernel and hence the quadratic confinement contributes to the interaction between mesons. This is a non-trivial result that can be compared with the baryon-baryon interaction where Refs. [57, 58] report the quark-exchange kernel generated by purely quadratic confinement being proportional to the norm kernel and thus in this case the quadratic confinement does not contribute to (the baryon baryon) interaction. If confinement contributes to the meson-meson interaction, it may worsen the van der Waals force problem between isolated mesons that results by a sum of the two-body potential, but this is against the empirical evidence. But, as mentioned in the Introduction, we are finding meson level dynamical implications of the quark potential model improvements [14, 15, 17] that use multi-quark interactions in form of the f factor to avoid this problem; many works, including Ref. [59], closely related to Ref. [57], had earlier suggested that a many-body interaction is needed to avoid this long range interaction between mesons.

Using all the kernels, we get two integral equations for $k=1,2$; we write here one of them:

$$\Big[\frac{3}{4}(\omega_{21}+\omega_{22})-\frac{s_2}{2m}\nabla^2_{\boldsymbol{R}_2}-\frac{8}{3}\bar{C}-4C[d^2_{21}+d^2_{22}]$$
$$+2m(r+1)-E_c\Big]\chi_2(\boldsymbol{R}_2)$$
$$+l_0\int \mathrm{d}^3\boldsymbol{R}_1\Big[-\frac{1}{2m}\frac{1}{6}\Big[r_{21}\boldsymbol{R}^2_1+r_{22}\boldsymbol{R}^2_2+r_{20}\Big]$$
$$+\frac{1}{2}\Big[n_1\boldsymbol{R}^2_1+n_0\Big]-\frac{1}{6}\Big(E_c+\frac{8}{3}\bar{C}-2m(r+1)\Big)\Big]$$
$$\exp(-l_1\boldsymbol{R}^2_1-l_2\boldsymbol{R}^2_2)\chi_1(\boldsymbol{R}_1)=0. \tag{22}$$

Here s_2, ω's, l's, n's and r's depend upon the constituent quark masses, sizes of mesons, the parameter k_f and b_s; see Appendix. It is clear from this equation that off-diagonal parts vanish for large values of $\boldsymbol{R}_1$ and $\boldsymbol{R}_2$. With no interaction in this limit between the two mesons, the total center of mass energy in the large separation limit will be the sum of kinetic energies of the relative motion of mesons and masses of the two mesons. This gives an alternative mesonic form for the diagonal terms surviving at large distance (no interaction limit), which can be utilized to write our integral equations as

$$\Big[M_{\mathrm{x}}+M_{\mathrm{J}/\psi}-\frac{1}{2\mu_{\mathrm{xJ}/\psi}}\nabla^2_{\boldsymbol{R}_2}-E_c\Big]\chi_2(\boldsymbol{R}_2)$$
$$+l_0\int \mathrm{d}^3\boldsymbol{R}_1\Big[-\frac{1}{2m}\frac{1}{6}\Big[r_{21}\boldsymbol{R}^2_1+r_{22}\boldsymbol{R}^2_2+r_{20}\Big]$$
$$+\frac{1}{2}\Big[n_1\boldsymbol{R}^2_1+n_0\Big]-\frac{1}{6}\Big(E_c+\frac{8}{3}\bar{C}-2m(r+1)\Big)\Big]$$
$$\exp(-l_1\boldsymbol{R}^2_1-l_2\boldsymbol{R}^2_2)\chi_1(\boldsymbol{R}_1)=0, \tag{23}$$

with x = ω,ρ, and a similar one with the diagonal term as $\Big[M_D+M_{\bar{D}^{0*}}-\dfrac{1}{2\mu_{\bar{D}^0\bar{D}^{0*}}}\nabla^2_{\boldsymbol{R}_1}-E_c\Big]$. By taking the Fourier transform of Eq. (23), we get

$$\Big[M_{\mathrm{x}}+M_{\mathrm{J}/\psi}+\frac{1}{2\mu_{\mathrm{xJ}/\psi}}\boldsymbol{P}^2_2-E_c\Big]\chi_2(\boldsymbol{P}_2)$$
$$-\frac{1}{2m}\frac{r_{22}}{6}A_1(l_1)F_b(\boldsymbol{P}_2,l_2)$$
$$+\Big[\Big(-\frac{1}{2m}\frac{r_{20}}{6}+\frac{n_0}{2}-\frac{E'_c}{6}\Big)A_1(l_1)$$
$$+\Big(-\frac{1}{2m}\frac{r_{21}}{6}+\frac{n_1}{2}\Big)B_1(l_1)\Big]F_a(\boldsymbol{P}_2,l_2)=0. \tag{24}$$

where $E_c' = E_c + \frac{8}{3}\bar{C} - 2m(r+1)$. In these equations

$$A_k(u) = l_0 \int \mathrm{d}^3\boldsymbol{R}_k \exp[-u\boldsymbol{R}_k^2]\chi_k(\boldsymbol{R}_k) \tag{25}$$

$$B_k(u) = l_0 \int \mathrm{d}^3\boldsymbol{R}_k \exp[-u\boldsymbol{R}_k^2]\boldsymbol{R}_k^2\chi_k(\boldsymbol{R}_k) \tag{26}$$

$$\begin{aligned} F_a(\boldsymbol{P}_k,u) &\equiv \int \frac{\mathrm{d}^3\boldsymbol{R}_k}{(2\pi)^{\frac{3}{2}}}\exp[i\boldsymbol{P}_k.\boldsymbol{R}_k]\exp[-u\boldsymbol{R}_k^2] \\ &= \frac{1}{(2u)^{\frac{3}{2}}}\exp\left[-\frac{\boldsymbol{P}_k^2}{4u}\right] \end{aligned} \tag{27}$$

$$\begin{aligned} F_b(\boldsymbol{P}_k,u) &\equiv \int \frac{\mathrm{d}^3\boldsymbol{R}_k}{(2\pi)^{\frac{3}{2}}}\exp[i\boldsymbol{P}_k.\boldsymbol{R}_k]\boldsymbol{R}_k^2\exp[-u\boldsymbol{R}_k^2] \\ &= F_a(\boldsymbol{P}_k,u)\left[\frac{1}{2u}\right]\left[3-\frac{\boldsymbol{P}_k^2}{2u}\right]. \end{aligned} \tag{28}$$

For the incoming waves in the first channel, our two integral equations (Eq. (24) and the other one; we *now* write both) can be formally solved [16] as (see Appendix B for details)

$$\chi_1(p_1) = \frac{\delta(p_1-p_c(1))}{p_c^2(1)} - \frac{1}{\Delta_1(p_1)}\Big[W_1^{(1)}A_2(l_2)+W_2^{(1)}B_2(l_2)\Big] \tag{29}$$

$$\chi_2(p_2) = -\frac{1}{\Delta_2(p_2)}\Big[W_1^{(2)}A_1(l_1)+W_2^{(2)}B_1(l_1)\Big]. \tag{30}$$

Here

$$\Delta_1(p_1) = \frac{p_1^2}{2\mu_{\mathrm{D}^0\bar{\mathrm{D}}^{0*}}} + M_{\mathrm{D}^0} + M_{\bar{\mathrm{D}}^{0*}} - E_c - i\epsilon \tag{31}$$

for an infinitesimal ϵ. Similarly,

$$\Delta_2(p_2) = \frac{p_2^2}{2\mu_{\mathrm{x}\mathrm{J}/\psi}} + M_{\mathrm{x}} + M_{\mathrm{J}/\psi} - E_c - i\epsilon \tag{32}$$

$$p_c(1) = \sqrt{2\mu_{\mathrm{D}^0\bar{\mathrm{D}}^{0*}}(E_c - M_{\mathrm{D}^0} - M_{\bar{\mathrm{D}}^{0*}})} \tag{33}$$

$$p_c(2) = \sqrt{2\mu_{\mathrm{x}\mathrm{J}/\psi}(E_c - M_{\mathrm{x}} - M_{\mathrm{J}/\psi})}. \tag{34}$$

$$\begin{aligned} W_1^{(1)} &= \Big[-\frac{1}{2m}\frac{r_{11}}{6}+\frac{n_1}{2}\Big]F_b(p_c(1),l_1) \\ &\quad +\Big[-\frac{1}{2m}\frac{r_{10}}{6}+\frac{n_0}{2}-\frac{E_c'}{6}\Big]F_a(p_c(1),l_1) \end{aligned} \tag{35}$$

$$W_2^{(1)} = -\frac{1}{2m}\frac{r_{12}}{6}F_a(p_c(1),l_1) \tag{36}$$

$$\begin{aligned} W_1^{(2)} &= -\frac{1}{2m}\frac{r_{22}}{6}F_b(p_c(2),l_2) \\ &\quad +\Big[-\frac{1}{2m}\frac{r_{20}}{6}+\frac{n_0}{2}-\frac{E_c'}{6}\Big]F_a(p_c(2),l_2) \end{aligned} \tag{37}$$

$$W_2^{(2)} = \Big[-\frac{1}{2m}\frac{r_{21}}{6}+\frac{n_1}{2}\Big]F_a(p_c(2),l_2). \tag{38}$$

From Eqs. (29) and (30) we can read off the T-matrix elements T_{11} and T_{21} [16] as co-efficients of Green's function operators $-\frac{1}{\Delta_1(p_1)}$ and $-\frac{1}{\Delta_2(p_2)}$ respectively. So, we have

$$T_{11} = 2\mu_{\mathrm{D}^0\bar{\mathrm{D}}^{0*}}\frac{\pi}{2}p_c(1)\Big[W_1^{(1)}A_2(l_2)+W_2^{(1)}B_2(l_2)\Big] \tag{39}$$

$$T_{21} = 2\mu_{\mathrm{x}\mathrm{J}\psi}\frac{\pi}{2}p_c(1)\sqrt{\frac{v_2}{v_1}}\Big[W_1^{(2)}A_1(l_1)+W_2^{(2)}B_1(l_1)\Big], \tag{40}$$

where $v_1 = p_c(1)/\mu_{\mathrm{D}^0\bar{\mathrm{D}}^{0*}}$ and $v_2 = p_c(2)/\mu_{\mathrm{x}\mathrm{J}\psi}$. Similarly T_{22} and T_{12} can be found for the incoming waves in the 2nd channel, with the V_2 in Appendix B changed accordingly. These are

$$T_{22} = 2\mu_{\mathrm{x}\mathrm{J}\psi}\frac{\pi}{2}p_c(2)\Big[W_1^{(2)}A_1(l_1)+W_2^{(2)}B_1(l_1)\Big] \tag{41}$$

$$T_{12} = 2\mu_{\mathrm{D}^0\bar{\mathrm{D}}^{0*}}\frac{\pi}{2}p_c(2)\sqrt{\frac{v_1}{v_2}}\Big[W_1^{(1)}A_2(l_2)+W_2^{(1)}B_2(l_2)\Big]. \tag{42}$$

4 Parameter fixing

At the quark level we adopt the model of Refs. [14, 15], that includes the parameters k_f and b_s in the gluonic field overlap factor f. We take the value of $k_f = 0.075$ [15] and b_s as 0.18 GeV^2 [55]. Our own contribution is in using the meson wave functions to find the hadron level implications for our chosen channels. These are eigenfunctions of potential of Eq. (4) which has parameters C and $\bar{C}$, whose numerical values we find by equating relevant terms in the large distance limit of Eq. (22) to the J/ψ meson mass; see Eq. (23). This gives

$$M_{\mathrm{J}/\psi} = \frac{3}{4}\omega_{22} - \frac{4}{3}\bar{C} - 4Cd_{22}^2 + 2m_{\mathrm{c}}. \tag{43}$$

Comparing Eqs. (10) and (4) with the standard form of potential of a simple harmonic oscillator gives $-4C/3 = \mu_{\mathrm{c}\bar{\mathrm{c}}}\omega_{22}^2/2$. Using this and $\omega_{22} = 1/m_c d_{22}^2$, we can eliminate C and the size d_{22} in favor of ω_{22} to get

$$M_{\mathrm{J}/\psi} = \frac{3}{2}\omega_{22} - \frac{4}{3}\bar{C} + 2m_{\mathrm{c}}. \tag{44}$$

This equation tells that in our model the dynamics of quarks, incorporating the effects of the gluonic field in the form of the potential, causes the mass of the quark antiquark cluster (a meson) to be a few percent different to the mere sum $2m_{\rm c}$ of quark masses. Our choice in Eq. (4) of using a simple harmonic oscillator potential with a known total energy allows us to write kinetic energy as known total energy minus potential energy. Thus the origin of clustering, or charm-anticharm quark binding, is in the parameters C and $\bar{C}$ of the potential in Eq. (4). The factor $-\frac{4}{3}$ in Eq. (44) multiplying $\bar{C}$ is a color factor which is the color expectation value of the $\boldsymbol{F}_i\cdot\boldsymbol{F}_j$ operator in Eq. (3). We have defined C by $-4C/3=\mu_{c\bar{c}}\omega_{22}^2/2$ with positive ω_{22}, making C to be negative. Below we replace C by ω_{22} as our model parameter.

There is no spin dependence in this modeled origin of the quark-antiquark clustering or binding; our neglect of the hyperfine interaction is responsible for this spin-independence. Thus, we do not make separate models of two different spin states of otherwise one quark-antiquark clustering of, say, a specified angular momentum between a quark and an antiquark. Specifically, this means that we are not able to model the mass difference of J/ψ($1S$) and η_c which have the same quark antiquark angular momentum $L=0$ and differ only in spin dependence. Thus we fit our remaining parameters ω_{22} and $\bar{C}$, mentioned in the above paragraph, to the spin averaged masses of charmonium in the state $1S$ and the state $2S$. This replaces Eq. (44) by

$$\frac{3M_{\rm J/\psi}(1S)+M_{\eta_{\rm c}}(1S)}{4}=\frac{3}{2}\omega_{22}-\frac{4}{3}\bar{C}+2m_{\rm c}. \tag{45}$$

For a comparison, Ref. [60] uses the spin averaged $\bar{b}b$ spectrum in its Fig. 1. An explicit formula for spin averaged mass can be seen as Eq. (3.1) of Ref. [61].

For the 2S state, 3/2 is replaced by 7/2 because of the 3-d S.H.O. $E_{nlm}=\omega_{22}(4n+2l+3)/2$ [62], for this $n=1$ and $l=0$. The corresponding equation is

$$\frac{3M_{\rm \Psi}(2S)+M_{\eta_{\rm c}}(2S)}{4}=\frac{7}{2}\omega_{22}-\frac{4}{3}\bar{C}+2m_{\rm c}. \tag{46}$$

Setting the values of masses $M_{\rm J/\psi}(1S)=3.0969$ GeV, $M_{\eta_{\rm c}}(1S)=2.9803$ GeV, $M_{\rm \Psi}(2S)=3.6861$ GeV and $M_{\eta_{\rm c}}(2S)=3.6370$ GeV from (PDG) Ref. [63] in Eqs. (45) and (46) and solving them simultaneously, we get $\bar{C}=0.2592$ GeV and $\omega_{22}=0.3030$ GeV for a charm-anticharm cluster. We use the constituent quark masses values $m_{\rm c}=1.4794$ GeV and $m=0.33$ GeV (for light quarks) from Ref. [52]. For the angular frequencies $\omega's$ and hence sizes of heavy-light and light-light clusters, we used the S.H.O. property that size squared is inversely proportional to the square root of the relevant reduced mass (that is of the quark and antiquark in the meson).

5 Results and conclusion

According to Eqs. (39), (40), (41) and (42), the T-matrix elements are given in terms of the elements of V_1 and V_2 column matrices which satisfy the inhomogeneous equation Eq. (B7). These solutions of Eq. (B7) are finite if $\mathtt{det}W\neq 0$. Using the numerical values of our parameters, we calculate the T matrix elements as a function of energy, which in turn give the spin averaged cross-sections using the following relation [64]

$$\sigma_{ii'}=\frac{4\pi}{p_c^2(i')}\sum_J\frac{(2J+1)}{(2s_1+1)(2s_2+1)}|T_{ii'}|^2, \tag{47}$$

where J is the total angular momentum of the mesons and s_1 and s_2 are the spin of the two incoming mesons. (For the definition of $p_c^2(i')$, see Eqs. (33) and (34) above.) Here $i,i'=1,2$ label our channels. In Fig. 3 we show the spin averaged cross sections versus $T_{\rm c}=E_{\rm c}-M_{\bar{\rm D}^0}-M_{\rm D^{0*}}$ for the process $\bar{\rm D}^0{\rm D}^{0*}\longrightarrow\bar{\rm D}^0{\rm D}^{0*}$ and $T_{\rm c}=E_{\rm c}-M_{\omega}-M_{\rm J/\psi}$ for the processes $\bar{\rm D}^0{\rm D}^{0*}\longrightarrow\omega{\rm J/\psi}$, $\omega{\rm J/\psi}\longrightarrow\bar{\rm D}^0{\rm D}^{0*}$ and $\omega{\rm J/\psi}\longrightarrow\omega{\rm J/\psi}$ for the QCD-based model that we are using, which means the parameter k_f is taken as 0.075. The cross sections are smooth (without any peak), relatively small and decrease very rapidly with $T_{\rm c}$. In Fig. 4 the cross sections of the same processes are given for the sum of two-body potential model, that is setting the value of the parameter k_f as zero. The cross sections in this case are smooth, relatively large and again decrease rapidly with $T_{\rm c}$. To find the cross sections of the processes given in Figs. 3 and 4, we assume that channels 1 and 2 are $\bar{\rm D}^0{\rm D}^{0*}$ and $\omega{\rm J/\psi}$ respectively. However, if channel 2 is taken as $\rho{\rm J/\psi}$ then we can obtain the cross sections of the processes $\bar{\rm D}^0{\rm D}^{0*}\longrightarrow\bar{\rm D}^0{\rm D}^{0*}$, $\bar{\rm D}^0{\rm D}^{0*}\longrightarrow\rho{\rm J/\psi}$, $\rho{\rm J/\psi}\longrightarrow\bar{\rm D}^0{\rm D}^{0*}$ and $\rho{\rm J/\psi}\longrightarrow\rho{\rm J/\psi}$. Here $T_{\rm c}=E_{\rm c}-M_{\rho}-M_{\rm J/\psi}$ for all the processes excluding the process $\bar{\rm D}^0{\rm D}^{0*}\longrightarrow\bar{\rm D}^0{\rm D}^{0*}$, where we have taken $T_{\rm c}=E_{\rm c}-M_{\bar{\rm D}^0}-M_{\rm D^{0*}}$. The plots of these cross sections are given in Figs. 5 and 6 for $k_f=0.075$ and 0 respectively. We again find that the cross sections are suppressed when the Gaussian f factor is included. The first process $\bar{\rm D}^0{\rm D}^{0*}\longrightarrow\bar{\rm D}^0{\rm D}^{0*}$, which is common in both sets of processes, was found to have the same cross section whereas the values of cross sections of other processes are somewhat different.

At $\det W=0$ the solution of Eq. (B7) diverges, which corresponds to a pole of scattering amplitude and represents a bound state (resonance) with respect to a given process if its energy is less (greater) than the process threshold which is equal to the total rest mass of the final (inital) particles in case of endothermic (exothermic) processes respectively. In order to calculate the energy where the pole exists for our $\rm q^2\bar{q}^2$ system we simply have to solve $\det W=0$ for the energy variable. We find that

$\mathtt{det}W \neq 0$ for all $T_c > 0$ when $k_f = 0$ and $k_f = 0.075$. These results are consistent with the plots in Figs. 3–6 of the cross sections in which no resonating peak appears for these values of k_f.

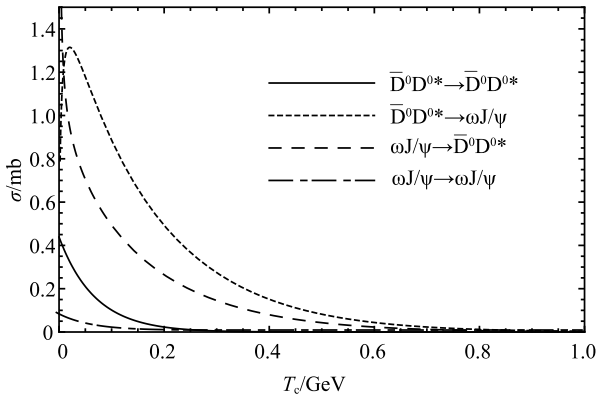

Fig. 3. Total spin averaged cross sections for Gaussian form of f with $k_f = 0.075$ versus T_c when channel 2 is taken as $\omega J/\psi$.

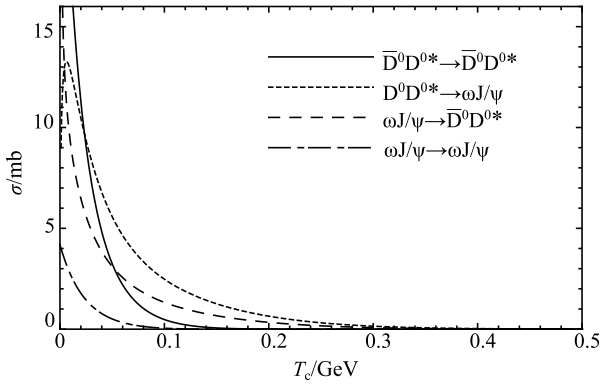

Fig. 4. Total spin averaged cross sections for $k_f = 0$ versus T_c when channel 2 is taken as $\omega J/\psi$.

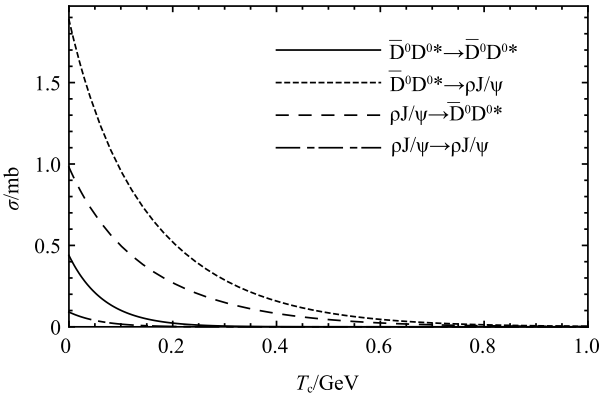

Fig. 5. Total spin averaged cross sections for Gaussian form of f with $k_f = 0.075$ versus T_c when channel 2 is taken as $\rho J/\psi$.

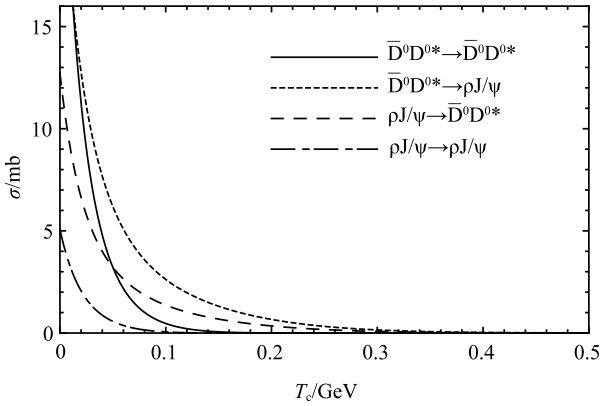

Fig. 6. Total spin averaged cross sections for $k_f = 0$ versus T_c when channel 2 is taken as $\rho J/\psi$.

As Refs. [33–38] have pointed out that $\bar{D}^0D^{0*}$ may form a bound state, it is worth examining if by changing the strength of our interaction we can get a meson-meson bound state or resonance. To do this analysis we introduce a parameter I_0 as in Ref. [50], changing the net strength of our meson-meson interaction. Physically, this parameter I_0 tells how far we are from getting a bound state at 3872 MeV if we study only one component $\bar{D}^0D^{0*}$ of the full exotic meson X(3872) along with using other approximations. Any deviation of I_0 from 1 suggests how much can we improve modeling of this exotic meson. We implemented this re-scaling of the interaction strength by multiplying the off-diagonal terms of our potential, kinetic energy, and normalization matrices by l_0. For this, we multiplied l_0 from Eq. (22) and the other coupled integral equation by I_0. A value of I_0 away from 1 (for all the above results) changes the energy where condition $\det W = 0$ is satisfied. The energy of the bound state generally depends on the strength parameter I_0 of the interaction in two possible ways [65]; either the energy of the bound state increases or decreases with the strength parameter. In the former case it is usually called a virtual state whereas in the latter case we call it a proper bound state. In Fig. 7 we show the dependence of the c.m. energy at pole on the strength parameter I_0, subject to the constraint $\det W = 0$, by different curves for $k_f = 0$, 0.05, 0.075, and 0.1 respectively. While solving $\det W = 0$ we note that the solution can be obtained conveniently if we put the value of E_c and other kinematical variables and solve it for I_0 rather than solving it for E_c. In this way we find that the resultant equation is quadratic in I_0, which means we may have two values of I_0 corresponding to one value of E_c. However, we find that one of the two roots is always complex and the real root is found to be a continuous function of E_c, as indicated by the continuous curves in Fig. 7, in which solid and dashed segments correspond to the first and second real root respectively. These curves show that corresponding to each k_f, the resonance energy E_c

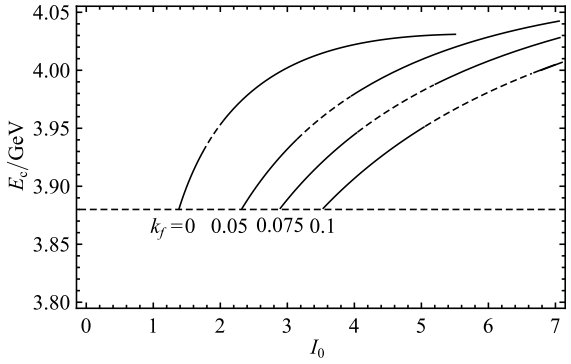

Fig. 7. Total centre of mass energy at pole versus strength parameter I_0, for different values of k_f, for the 2nd channel being $\omega J/\Psi$.

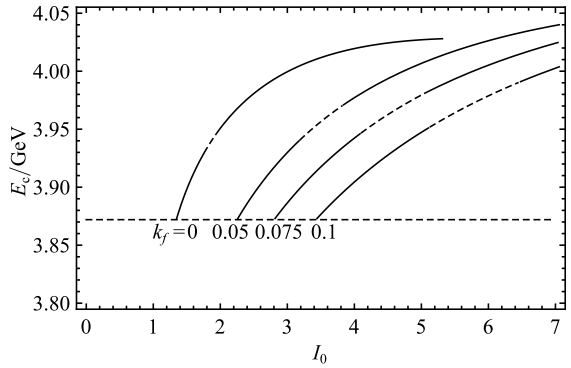

Fig. 8. Total centre of mass energy at pole versus strength parameter I_0, for different values of k_f, for the 2nd channel being $\rho J/\Psi$.

Table 1. Critical I_0 for different values of k_f.

	channel 2 ($\omega J/\psi$)	channel 2 ($\rho J/\psi$)
k_f	critical I_0	critical I_0
0	1.3863	1.3487
0.05	2.3253	2.2610
0.075	2.8950	2.8164
0.1	3.5357	3.4422

increases with I_0 provided that I_0 is greater than a critical value, which depends on the value of k_f. For example for $k_f = 0.075$ the critical $I_0 = 2.89$ for the 2nd channel being $\omega J/\psi$. It means that the pole of the scattering amplitude does not exist at $I_0 < 2.89$ when the f factor is included at $k_f = 0.075$. Similarly for $k_f = 0$ the critical $I_0 = 1.38$. This explains why no resonating peak appears in the plots of the cross sections when I_0 is taken as 1, irrespective of the value of k_f. The curves given in Fig. 7 are produced by assuming that channels 1 and 2 are $\bar{\mathrm{D}}^0\mathrm{D}^{0*}$ and $\omega J/\psi$ respectively. We find similar results when channel 2 is taken as $\rho J/\psi$, as shown in Fig. 8. In Table 1 we give the critical values of I_0 corresponding to different values of k_f for the two choices of channel 2. It is also noted that the minimum E_c at which $\det W = 0$ is 3.881 and 3.872 GeV for channel 2 being $\omega J/\psi$ and $\rho J/\psi$ respectively, irrespective of the value of k_f. These values are slightly greater than or equal to $m_{\mathrm{D}^0} + m_{\mathrm{D}^{*0}}$ (3.872 GeV), $m_\omega + m_{\mathrm{J}/\psi}$ (3.88 GeV), and $m_\rho + m_{\mathrm{J}/\psi}$ (3.872 GeV). This implies that in our case the pole of the scattering amplitude corresponds to a resonance in the system. Thus, we conclude that the $\mathrm{c\bar{c}u\bar{u}}$ system cannot resonate whether we assume the sum of two-body approach (i.e., $k_f = 0$) or include QCD effects in terms of gluonic field overlap factor f at $I_0 = 1$. However, the resonance may be produced if the interaction strength I_0 is increased by at least a factor of 1.38 (1.35) and 2.89 (2.82) for $k_f = 0$ and 0.075 respectively when channel 2 is $\omega J/\psi$ ($\rho J/\psi$). It is tempting to associate the resonance in $\mathrm{q^2\bar{q}^2}$ with the $\bar{\mathrm{D}}^0\mathrm{D}^{0*}$ component of X(3872). The result that this resonance appears only when interaction strength parameter I_0 is greater than a critical value may be related to the use of various approximations used in this work, including ignoring the annihilation effects of light quark flavors and using quadratic confinement. As for the full X(3872), our neglect of its $\mathrm{c\bar{c}}$ component [26–32] may also be responsible for deviation of the parameter I_0 away from 1. If future improvements beyond our approximations are equivalent to an effective I_0 that is less than one, our work would imply that $\bar{\mathrm{D}}^0\mathrm{D}^{0*}$ does not form a bound state and hence there can not be a role for the $\bar{\mathrm{D}}^0\mathrm{D}^{0*}$ molecule in the structure of X(3872). If the resulting effective I_0 is increased beyond the critical values mentioned in Table 1, the $\bar{\mathrm{D}}^0\mathrm{D}^{0*}$ bound state may represent X(3872).

6 Conflicts of interest

The authors declare that there is no conflict of interest regarding the publication of this manuscript.

Appendix A

Here we show how we perform the spatial integrations on the left hand side of Eqs. (19–21) to read our kernels. From Figs. (1) and (2) we see that $\boldsymbol{y}_1, \boldsymbol{z}_1$, $\boldsymbol{R}_1$ and $\boldsymbol{y}_2, \boldsymbol{z}_2$, $\boldsymbol{R}_2$ form two linearly independent sets. Thus for the diagonal terms $k = l$ in Eq. (8), $\chi_l(\boldsymbol{R}_l)$ can be taken outside the integration on the RHS of Eq. (21). Thus, normalization of $\xi_k(\boldsymbol{y}_k)$,

defined in Eq. (7) and a similar $\zeta_k(\boldsymbol{z}_k)$, gives

$$\int \mathrm{d}^3\boldsymbol{R}'_k \boldsymbol{N}_{kk}(\boldsymbol{R}_k,\boldsymbol{R}'_k)\chi_k(\boldsymbol{R}'_k)=\chi_k(\boldsymbol{R}_k) \quad \text{or} \tag{A1}$$

$$\boldsymbol{N}_{kk}(\boldsymbol{R}_k,\boldsymbol{R}'_k)=\delta(\boldsymbol{R}_k,\boldsymbol{R}'_k). \tag{A2}$$

For kinetic energy, in Eq. (11) we can write for $k=1$ or $k=2$

$$\left(\sum_{i=1}^{\overline{4}}-\frac{\nabla_i^2}{2m_i}\right)=-\frac{1}{2m}[s_k\underline{\nabla^2_{\boldsymbol{R}_k}}+q_k\underline{\nabla^2_{\boldsymbol{y}_k}}+t_k\underline{\nabla^2_{\boldsymbol{z}_k}}], \tag{A3}$$

with m the constituent mass of the light quark, up or down and

$$s_1=\frac{2}{r+1},\ \ q_1=t_1=\frac{r+1}{r},\ \ s_2=\frac{r+1}{2r},\ \ q_2=2,\ \ t_2=\frac{2}{r}. \tag{A4}$$

By using Eq. (A3) in Eq. (19) and doing the required space differentiations and integrations, we get

$$\boldsymbol{K}_{kk}(\boldsymbol{R}_k,\boldsymbol{R}'_k)=\delta(\boldsymbol{R}_k,\boldsymbol{R}'_k)\left[\frac{3}{4}(\omega_{k1}+\omega_{k2})-\frac{s_k}{2m}\underline{\nabla^2_{\boldsymbol{R}_k}}\right] \quad \text{with} \tag{A5}$$

$$\omega_{k1}=\frac{q_k}{2md^2_{k1}} \text{ and } \omega_{k2}=\frac{t_k}{2md^2_{k2}}. \tag{A6}$$

For the potential energy matrix, by using Eqs. (4) and (10) we get

$$V_{kk}=-\frac{4}{3}\Big[2\bar{C}+C\boldsymbol{y}_k^2+C\boldsymbol{z}_k^2\Big]. \tag{A7}$$

Using this in Eq. (20) and doing the required integrations, we get

$$\boldsymbol{V}_{kk}(\boldsymbol{R}_k,\boldsymbol{R}'_k)=\delta(\boldsymbol{R}_k,\boldsymbol{R}'_k)\Big[-\frac{8}{3}\bar{C}-4C[d^2_{k1}+d^2_{k2}]\Big]. \tag{A8}$$

Now for the off-diagonal elements we have to replace $\boldsymbol{y}_1$ and $\boldsymbol{z}_1$ by $\boldsymbol{R}_2$ and $\boldsymbol{g}_1$, where

$$\boldsymbol{g}_1=\boldsymbol{y}_1+\boldsymbol{z}_1. \tag{A9}$$

Only $\boldsymbol{g}_1$ is integrated. The rest is a function of $\boldsymbol{R}_2$ and $\boldsymbol{R}_1$ (constant in this integration). Similarly we replace $\boldsymbol{y}_2$ and $\boldsymbol{z}_2$ by $\boldsymbol{R}_1$ and $\boldsymbol{g}_2$, where

$$\boldsymbol{g}_2=\boldsymbol{y}_2+r\boldsymbol{z}_2. \tag{A10}$$

Only $\boldsymbol{g}_2$ is integrated. The rest is a function of $\boldsymbol{R}_1$ and $\boldsymbol{R}_2$ (constant in this integration). We get from Eqs. (9), (2), (21) after doing all the integrations other than $\boldsymbol{R}_l$

$$\boldsymbol{N}_{12}(\boldsymbol{R}_1,\boldsymbol{R}_2)=\boldsymbol{N}_{21}(\boldsymbol{R}_2,\boldsymbol{R}_1)=\frac{l_0}{3\sqrt{2}}\exp(-l_1\boldsymbol{R}_1^2-l_2\boldsymbol{R}_2^2). \tag{A11}$$

Here

$$l_0=(r+1)^{\frac{9}{4}}r^{\frac{-15}{8}}2^{\frac{3}{4}}(\pi\alpha d^2)^{\frac{-3}{2}} \tag{A12}$$

$$l_1=\frac{1}{4d^2}\Big(\frac{r+1}{2}\Big)^2\Big[\gamma-\frac{\beta^2}{\alpha}\Big] \tag{A13}$$

$$l_2=4\bar{k}+\frac{1}{2d^2}\sqrt{\frac{2r}{r+1}} \tag{A14}$$

where $\bar{k}=k_f b_s$,

$$\alpha=8\bar{k}d^2\Big[\frac{r^2+1}{r^2}\Big]+1+r^{\frac{-3}{2}}\left[\frac{(r+1)^2}{\sqrt{2(r+1)}}+1\right] \tag{A15}$$

$$\beta=8\bar{k}d^2\Big[\frac{r^2-1}{r^2}\Big]+1+r^{\frac{-3}{2}}\left[\frac{r^2-1}{\sqrt{2(r+1)}}-1\right] \tag{A16}$$

$$\gamma=8\bar{k}d^2\Big[\frac{r^2+1}{r^2}\Big]+1+r^{\frac{-3}{2}}\left[\frac{(r-1)^2}{\sqrt{2(r+1)}}+1\right]. \tag{A17}$$

Now for the off-diagonal kinetic energy kernel, Eq. (11) gives

$$K_{kl}=\frac{1}{3}\sqrt{f}\left(\sum_{i=1}^{\overline{4}}-\frac{\nabla_i^2}{2m_i}\right)\sqrt{f}. \tag{A18}$$

Substituting in Eq. (19) and using Eq. (A9) and Eq. (A10), we get

$$\boldsymbol{K}_{12}(\boldsymbol{R}_1,\boldsymbol{R}_2)=-\frac{l_0}{2m}\frac{1}{3\sqrt{2}}\Big[r_{11}\boldsymbol{R}_1^2+r_{12}\boldsymbol{R}_2^2+r_{10}\Big]\exp(-l_1\boldsymbol{R}_1^2-l_2\boldsymbol{R}_2^2) \tag{A19}$$

$$\boldsymbol{K}_{21}(\boldsymbol{R}_2,\boldsymbol{R}_1)=-\frac{l_0}{2m}\frac{1}{3\sqrt{2}}\Big[r_{21}\boldsymbol{R}_1^2+r_{22}\boldsymbol{R}_2^2+r_{20}\Big]\exp(-l_1\boldsymbol{R}_1^2-l_2\boldsymbol{R}_2^2) \tag{A20}$$

where

$$\begin{aligned}r_{11}=&\Big(\frac{r+1}{2}\Big)^4\left[\frac{8(r-1)^2}{(r+1)^3}\left\{\Big(\frac{r-1}{r+1}\Big)\Big(\frac{8\bar{k}}{(r-1)^2}+\frac{1+\sqrt{r}}{(r-1)^2d^2}\Big)\right.\right.\\&\left.-\Big(\frac{\beta}{\alpha}-\frac{r-1}{r+1}\Big)\Big(\frac{2\bar{k}}{r}+\frac{1}{2d^2\sqrt{r}(1+\sqrt{r})}\Big)\right\}^2\\&+\frac{32r}{(r+1)^3}\left\{\Big(\frac{r-1}{r+1}\Big)\Big(\frac{2\bar{k}}{r}+\frac{1}{2d^2\sqrt{r}(1+\sqrt{r})}\Big)\right.\\&\left.\left.-\Big(\frac{\beta}{\alpha}-\frac{r-1}{r+1}\Big)\Big(\bar{k}\frac{r^2+1}{r^2}+\frac{r^{-3/2}+1}{4d^2}\Big)\right\}^2\right]\end{aligned} \tag{A21}$$

$$\begin{aligned}r_{10}=&-\frac{3}{2}\left(\frac{r+1}{2}\right)^2\left\{8\frac{(r-1)^2}{(r+1)^3}\left(\frac{8\bar{k}}{(r-1)^2}+\frac{1+\sqrt{r}}{(r-1)^2d^2}\right)\right.\\&\left.+\frac{32r}{(r+1)^3}\left(\frac{\bar{k}(r^2+1)}{r^2}+\frac{r^{\frac{-3}{2}}+1}{4d^2}\right)\right\}\\&+\frac{3}{2}\frac{d^2}{\alpha}(r+1)^2\left\{\frac{8(r-1)^2}{(r+1)^3}\left(\frac{2\bar{k}}{r}+\frac{1}{2d^2\sqrt{r}\,(1+\sqrt{r})}\right)^2\right.\\&\left.+\frac{32r}{(r+1)^3}\left(\frac{\bar{k}(r^2+1)}{r^2}+\frac{r^{\frac{-3}{2}}+1}{4d^2}\right)^2\right\}\\&-\frac{6(r+1)}{2r}\left(2\bar{k}+\frac{1}{2d^2}\sqrt{\frac{2r}{r+1}}\right)\end{aligned} \tag{A22}$$

$$r_{12}=4\left(\frac{r+1}{2r}\right)\left(2\bar{k}+\frac{1}{2d^2}\sqrt{\frac{2r}{r+1}}\right)^2 \tag{A23}$$

$$r_{22}=r_{12} \tag{A24}$$

$$\begin{aligned}r_{20}=&\frac{8}{(r+1)^2}\Big(\frac{r+1}{2}\Big)^2\frac{24d^2}{\alpha}\left\{\Big(\bar{k}+\frac{1}{4d^2}\Big)^2+r\Big(\frac{\bar{k}}{r^2}+\frac{r^{-\frac{3}{2}}}{4d^2}\Big)^2\right\}\\&-6\frac{8}{(r+1)^2}\Big(\frac{r+1}{2}\Big)^2\left\{\Big(\bar{k}+\frac{1}{4d^2}\Big)+r\Big(\frac{\bar{k}}{r^2}+\frac{r^{-\frac{3}{2}}}{4d^2}\Big)\right\}\\&-6\frac{r+1}{2r}\left\{2\bar{k}+\frac{1}{2d^2}\sqrt{\frac{2r}{r+1}}\right\}\end{aligned} \tag{A25}$$

and

$$\begin{aligned}r_{21}=&2(r+1)^2\left\{\Big(1-\frac{\beta}{\alpha}\Big)^2\Big(\bar{k}+\frac{1}{4d^2}\Big)^2\right.\\&\left.+r\Big(1+\frac{\beta}{\alpha}\Big)^2\Big(\frac{\bar{k}}{r^2}+\frac{r^{\frac{-3}{2}}}{4d^2}\Big)^2\right\}.\end{aligned} \tag{A26}$$

Lastly, for the potential energy kernel with $k\neq l$, using Eqs. (4) and (10) in Eq. (20), changing variables and doing all the integrations, we get

$$\begin{aligned}&\boldsymbol{V}_{12}(\boldsymbol{R}_1,\boldsymbol{R}_2)=\boldsymbol{V}_{21}(\boldsymbol{R}_2,\boldsymbol{R}_1)\\&=l_0\Big[n_1\boldsymbol{R}_1^2+n_0\Big]\exp(-l_1\boldsymbol{R}_1^2-l_2\boldsymbol{R}_2^2),\end{aligned} \tag{A27}$$

with

$$n_0=-\frac{8}{3}C\left(\frac{r+1}{r}\right)^2\frac{d^2}{\alpha} \tag{A28}$$

$$n_1=-\frac{4}{9}C\left\{\frac{(r+1)^4}{4r^2}\right\}\left(\frac{\beta}{\alpha}-\frac{r-1}{r+1}\right)^2. \tag{A29}$$

Putting the expressions from Eqs. (A5), (A8), (A2), (A19), (A27) and (A11) in Eq. (18), we get the first integral equation for k=1 and by putting the expressions from Eqs. (A5), (A8), (A2), (A20), (A27) and (A11) in (18), we get the second integral equation for k =2, that we have shown as Eq. (22).

Appendix B

Because of the spherical symmetry of the S-wave ($l=0$), $\boldsymbol{P}_i$ is replaced with p_i (magnitude) with $i=1,2$. Using the Parseval relation, Eqs. (25) and (26) give

$$A_k(u)=4\pi l_0\int \mathrm{d}p_k p_k^2 F_a(p_k,u)\chi_k(p_k) \tag{B1}$$

$$B_k(u)=4\pi l_0\int \mathrm{d}p_k p_k^2 F_b(p_k,u)\chi_k(p_k). \tag{B2}$$

Multiplying Eq. (29) by $4\pi p_1^2 F_a(p_1,l_1)$ and integrating w.r.t. p_1 and using Eq. (B1) we get

$$\frac{A_1(l_1)}{l_0}=4\pi F_a(p_c(1),l_1)-A_2(l_2)W_{11}^{(1)}-B_2(l_2)W_{12}^{(1)} \tag{B3}$$

Similarly, multiplying Eq. (29) by $4\pi p_1^2 F_b(p_1,l_1)$ and integrating w.r.t. p_1 and using Eq. (B2), we get

$$\frac{B_1(l_1)}{l_0}=4\pi F_b(p_c(1),l_1)-A_2(l_2)W_{21}^{(1)}-B_2(l_2)W_{22}^{(1)} \tag{B4}$$

In the same way, multiplying Eq. (30) by $4\pi p_2^2 F_a(p_2,l_2)$ and $4\pi p_2^2 F_b(p_2,l_2)$ and integrating w.r.t. p_2 and using Eqs. (B1) and (B2), we get

$$\frac{A_2(l_2)}{l_0}=-A_1(l_1)W_{11}^{(2)}-B_1(l_1)W_{12}^{(2)} \tag{B5}$$

$$\frac{B_2(l_2)}{l_0}=-A_1(l_1)W_{21}^{(2)}-B_1(l_1)W_{22}^{(2)} \tag{B6}$$

where the W's in the above equations depend on the $l's, n's$, $r's$, E_c, $\bar{C}$ and the constituent quark mass of light quarks. Equations (B3), (B4), (B5) and (B6) can be written in matrix form as follows

$$WV_1=V_2 \tag{B7}$$

with

$$W=\begin{pmatrix} l_0^{-1} & 0 & W_{11}^{(1)} & W_{12}^{(1)}\\ 0 & l_0^{-1} & W_{21}^{(1)} & W_{22}^{(1)}\\ W_{11}^{(2)} & W_{12}^{(2)} & l_0^{-1} & 0\\ W_{21}^{(2)} & W_{22}^{(2)} & 0 & l_0^{-1}\end{pmatrix} \tag{B8}$$

$$V_1=\begin{pmatrix} A_1(l_1)\\ B_1(l_1)\\ A_2(l_2)\\ B_2(l_2)\end{pmatrix} \tag{B9}$$

$$V_2=4\pi\begin{pmatrix} F_a(p_c(1),l_1)\\ F_b(p_c(1),l_1)\\ 0\\ 0\end{pmatrix}. \tag{B10}$$

From Eq. (B7)), we can have

$$V_1=W^{-1}V_2 \tag{B11}$$

which gives the values of $A_1(l_1), B_1(l_1), A_2(l_2)$ and $B_2(l_2)$ needed in Eqs. (39) and (40).

References

1 J. Weinstein and N. Isgur, Phys. Rev. C, **27**: 588 (1983), J. Weinstein and N. Isgur, Phys. Rev. D, **41**: 2236 (1990)
2 T. Barnes and E. S. Swanson, Phys. Rev. D, **46**: 131 (1992)
3 Gui-Jun Ding, Wei Huang, Jia-Feng Liu, and Mu-Lin Yan, Phys. Rev. D, **79**: 034026 (2009)
4 E. S. Swanson, Phys. Lett. B, **588**: 189 (2004)
5 Ying Cui, Xiao-Lin Chen, Wei-Zhen Deng, and Shi-Lin Zhu, HighEnergyPhys. Nucl. Phys., **31**: 7 (2007)
6 T. Barnes, N. Black, and E. S. Swanson, Phys. Rev. C, **63**: 025204 (2001)
7 Cheuk-Yin Wong , E. S. Swanson, and T. Barnes, Phys. Rev. C, **62**: 045201 (2000)
8 Cheuk-Yin Wong , E. S. Swanson, and T. Barnes, Phys. Rev. C, **65**: 014903 (2002); **66**: 029901 (2002)
9 P. Bicudo, Nucl. Phys. A, **748**: 537 (2005)
10 E. S. Swanson, Phys. Rept. **429**, 243 (2006)
11 W. L. Wang,. F. Huang, Z.Y. Zhang et al, J. Phys. G, **34**: 1771 (2007)
12 Emiko Hiyama, Hideo Suganuma, and Masayasu Kamimura, Prog. Theor. Phys. Suppl., **168**: 101 (2007)
13 E. Hiyama, M. Kamimura, A. Hosaka et al, Phys. Lett. B, **633**: 237 (2006)
14 A. M. Green and P. Pennanen, Phys. Rev. C, **57**: 3384 (1998)
15 A. M. Green, J. Koponen, and P. Pennanen, Phys. Rev. D, **61**: 014014 (1999)
16 B. Masud, J. Paton, A. M. Green, and G. Q. Liu, Nucl. phys. A, **528**: 477 (1991)
17 A. M. Green and P. Pennanen, Phys. Lett. B, **426**: 243 (1998)
18 A.M.Green, C.Michael, M. E. Sainio, and Z. Phys. C, **67**: 291 (1995)
19 A.M.Green, J. Lukkarinen, P. Pennanen et al, Nucl. Phys. Proc. Suppl., **42**: 249 (1995)
20 A.M.Green, J.Lukkarinen, P. Pennanen et al, Phys. Rev. D, **53**: 261 (1996)
21 Petrus Pennanen, Phys. Rev. D, **55**: 3958 (1997)
22 Cheuk-Yin Wong, Phys. Rev. C, **69**: 055202 (2004)
23 Stephen Godfrey, arXiv: 0910.3409v2; Stephen Godfrey (Carleton), and Stephen L. Olsen (Hawaii and IHEP Beijing), Ann. Rev. Nucl. Part. Sci., **58**: 51 (2008), arXiv: 0801.3867
24 F. E. Close, Int.J.Mod.Phys. A, **20**: 5156 (2005) arXiv:hep-ph/0411396; J. Vijande, Int. J. Mod. Phys. A, **20**: 702 (2005), arXiv:hep-ph/0407136
25 Shi-Lin Zhu, Int. J. Mod. Phys. E, **17**, 283 (2008)
26 Yubing Dong, Amond Faessler, Thomas Gutsche, and Valery E Lyubovitskij, J. Phys. G, **38**: 015001 (2011)
27 P. G. Ortega, J. Segovia, D. R. Enten, and F. Fernendez, Phys. Rev. D, **81**: 0054023 (2010)
28 D. V. Bugg, J. Phys. G, **37**: 055002 (2010)
29 E. J. Eichten, K. Lane, and C. Quigg, Phys. Rev. D, **73**: 014014 (2006); **73**, 079903 (2006)
30 M. B. Voloshin, Int. J. Mod. Phys. A, **21**: 1239 (2006)
31 I. W. Lee, A. Faessler, T. Gutsche, and V. E. Lyubovitskij, Phys. Rev. D, **80**: 094005 (2009)
32 Yu. S. Kalashnikova and A. V. Nefediev, Phys. Rev. D, **80**: 074004 (2009)
33 E. S. Swanson, Phys. Lett. B, **598**: 197 (2004)
34 E. Braaten and Masaoki Kusunoki, Phys. Rev. D, **72**: 014012 (2005)
35 E. Braaten, Meng Lu, and Jungil Lee, Phys. Rev. D, **76**: 054010 (2007)
36 P. Colangelo, F. De Fazio, and S. Nicotri, Phys. Lett. B, **650**: 166 (2007)
37 Masayasu Harada, Yong-Liang Ma, and Prog. Theor. Phys., **126**: 91 (2011)
38 Thomas Mehan and Roxanne Springer, Phys. Rev. D, **83**: 094009 (2011)
39 Xiang Liu, Bo Zhang, and Shi-Lin Zhu, Phys. Lett. B, **645**: 185 (2007)
40 Ce Meng and Kuang-Ta Chao, Phys. Rev. D, **75**: 114002 (2007)
41 Eric Braaten, Masaoki Kusunoki, and Shmuel Nussinov, Phys. Rev. Lett., **93**: 162001 (2004)
42 Eric Braaten and Masaoki Kusunoki, Phys. Rev. D, **71**: 074005 (2005)
43 Eric Braaten, Daekyoung Kang, arXiv:1305.5564 [hep-ph] (2013)
44 T. Barnes, Eur. Phys. J. A, **18**: 531 (2003)
45 M. Imran Jamil, and Bilal Masud, Eur. Phys. J. A, **47**: 33 (2011)
46 T. Barnes, E. S. Swanson, and J. Weinstein, Phys. Rev. D, **46**: 4868 (1992)
47 T. Barnes and E. S. Swanson, Phys. Rev. C, **49**: 1166 (1994)
48 T. Barnes and NuovoCim. A, **107**: 2491 (1994)
49 S. M. Sohail Gilani, M. Imran Jamil, B. Masud, and Faisal Akram, work in progress
50 B. Masud, Phys. Rev. D, **50**: 6783 (1994)
51 W. R. Thomas, Phys. Rev. D, **41**: 3446 (1990)
52 T. Barnes, S. Godfrey, and E. S. Swanson, Phys. Rev. D, **72**: 054026 (2005)
53 S. Godfrey and N. Isgur, Phys. Rev. D, **32**: 189 (1985)
54 Bai-Qing Li and Kuang-Ta Chao, Phys. Rev. D, **79**: 094004 (2009)
55 Fumiko Okiharu, Hideo Suganuma, and Toru T. Takahashi, Phys. Rev. D, **72**: 014505 (2005)
56 K. Masutani, Nucl. Phys. A, **468**: 593 (1987)
57 Makota Oka and Koichi Yazaki, Progress of Theoretical Physics, **66** (2): 556 (1981)
58 J. Burger, R. Muller, K. Tragl, and H. M. Hofmann Nucl. Phys. A, **493**: 427 (1989)
59 Makota Oka and Koichi Yazaki, *Ch. 6, Quarks and Nuclei*, ed. by W. Weise, Singapore World Scientific, 1984
60 K. J. Juge, Phys. Rev. Letters, **82**: 4400 (1999)
61 L.C. Elliot, Master of Science Thesis Supervised by E. Swanson, North Carolina State Univesity, (1998)
62 Nouredine Zettili, *Quantum Mechanics*, (John Wiley and Sons, Ltd., 2001)
63 J. Beringer et al (Particle Data Group), Phys. Rev. D, **86**: 010001 (2012)
64 Steven Weinberg, *The Quantum Theory of Fields*, Vol-1 (Cambridge University Press, 2002)
65 J. R. Taylor, *Scattering Theroy: The Quantum Theory on Nonrelativistic Collisions* (John Wiley and Sons, 1972)